(2)

NRL Memorandum Report 5179

AD-A133 468

The Relation Between Power and Energy in the Shock Initiation of Detonations

I. Basic Theoretical Considerations and the Effects of Geometry

K. KAILASANATH* AND E. S. ORAN

Laboratory for Computational Physics

**Science Applications Inc.
McLean, VA 22102*

September 15, 1983

This work was supported by the Office of Naval Research.

NAVAL RESEARCH LABORATORY
Washington, D.C.

83 10 12 267

20000802031

SECURITY CLASSIFICATION OF THIS PAGE (When Data Entered)

REPORT DOCUMENTATION PAGE		READ INSTRUCTIONS BEFORE COMPLETING FORM
1. REPORT NUMBER NRL Memorandum Report 5179	2. GOVT ACCESSION NO. AD-A133 468	3. RECIPIENT'S CATALOG NUMBER
4. TITLE (and Subtitle) THE RELATION BETWEEN POWER AND ENERGY IN THE SHOCK INITIATION OF DETONATIONS I. Basic Theoretical Considerations and the Effects of Geometry		5. TYPE OF REPORT & PERIOD COVERED Interim report on a continuing NRL problem. 6. PERFORMING ORG. REPORT NUMBER
7. AUTHOR(s) K. Kailasanath* and E.S. Oran		8. CONTRACT OR GRANT NUMBER(s)
9. PERFORMING ORGANIZATION NAME AND ADDRESS Naval Research Laboratory Washington, DC 20375		10. PROGRAM ELEMENT, PROJECT, TASK AREA & WORK UNIT NUMBERS 44-1950-0-3
11. CONTROLLING OFFICE NAME AND ADDRESS		12. REPORT DATE September 15, 1983 13. NUMBER OF PAGES 45
14. MONITORING AGENCY NAME & ADDRESS(if different from Controlling Office)		15. SECURITY CLASS. (of this report) UNCLASSIFIED 15a. DECLASSIFICATION/DOWNGRADING SCHEDULE

16. DISTRIBUTION STATEMENT (of this Report)

Approved for public release; distribution unlimited.

17. DISTRIBUTION STATEMENT (of the abstract entered in Block 20, if different from Report)

18. SUPPLEMENTARY NOTES

*Present address: Science Applications Inc., McLean, VA 22102

This work was supported by the Office of Naval Research.

19. KEY WORDS (Continue on reverse side if necessary and identify by block number)

Detonation	Acetylene-oxygen mixtures
Minimum detonation energy	Detonation initiation

20. ABSTRACT (Continue on reverse side if necessary and identify by block number)

Recent studies on the direct initiation of gaseous detonations have shown that initiation depends not only on the energy deposited but also on the rate at which it is deposited, namely the power. In this paper, we have used a theoretical model to determine the relation between the power and the energy required for the initiation of planar, cylindrical and spherical detonations in a detonable gas mixture. The results from the model show that the qualitative differences in the power-energy

(Continues)

DD FORM 1 JAN 73 1473 EDITION OF 1 NOV 65 IS OBSOLETE
S/N 0102-014-6601

SECURITY CLASSIFICATION OF THIS PAGE (When Data Entered)

20. ABSTRACT (Continued)

relations obtained from two different experimental arrangements are due to differences in the geometry. We also show that the minimum power requirement corresponds to a shock of minimum Mach number only in the case of planar detonations. Finally, the effect on the power-energy relation of the ratio of specific heats and the experimental uncertainties in the determination of the induction times have been studied for an acetylene-oxygen-nitrogen mixture.

CONTENTS

THE RELATION BETWEEN POWER AND ENERGY IN THE SHOCK INITIATION OF DETONATIONS

I. Basic Theoretical Considerations and the Effects of Geometry

I. INTRODUCTION

The early studies of direct initiation of gaseous detonations[1,2,3] established the importance of the magnitude of the source energy. More recent experiments[4,5,6] have shown the importance not only of the energy but also of the rate at which the energy is deposited, namely the power. The experimental results of Lee et al.[5] indicate that there is a minimum detonation energy, E_m, below which a detonation would not occur no matter what the power is and that there is a minimum power, P_m, below which a detonation would not occur no matter what the total energy is. Later, they noted[6] that the requirement for a minimum value for the power of the source indicates that the source must be capable of generating a shock wave of certain minimum strength (Mach number). They also concluded that the minimum energy requirement implied that the shock wave must be maintained at or above this minimum strength for a certain minimum duration.

Recently these ideas have been used by Dabora[7,8] to obtain a relation between the power and energy required for the direct initiation of hydrogen-air detonations in a shock tube. However, this power-energy relation is very different qualitatively from those of Knystautas and Lee[6]. More recently Abouseif and Toong[9] have proposed a simple theoretical model to determine the power-energy relation and predict their respective threshold values. The predictions based on their model were in qualitative agreement with the experiments of Knystautas and Lee[5].

Manuscript approved June 22, 1983.

In this paper we have modified and extended the basic model proposed by Abouseif and Toong[9] and have used it to determine the relation between the power and the energy required for the initiation of planar, cylindrical and spherical detonations in a detonable gas mixture. Specifically, we discuss its application to a stoichiometric oxy-acetylene mixture. We have used the results from the model to explain the qualitative differences between the experimental results of Knystautas and Lee[6] and Dabora[7]. The relation between the minimum power requirement and the Mach number of the shock wave has also been examined. Some of the limitations of the model are discussed, and several applications are described.

II. THE THEORETICAL MODEL

We can, in principle, study the direct initiation of detonations by performing detailed numerical simulations of the flow field generated by a given source of energy. In general, such a calculation is a complicated, multidimensional, multispecies, time-dependent problem. Part of the complication and cost of such calculations arises from the solution of the conservation equations, and part of it arises from integrating the large number of ordinary differential equations describing the chemical reactions. This latter factor is further complicated by the fact that we usually do not have an adequate representation of the chemical reactions with which to work. Thus, a convenient, inexpensive way to evaluate the relative tendency of different explosive mixtures to detonate would be very useful. Below we develop and expand a simple theoretical model proposed earlier by Abouseif and Toong[9]. Although this approach is not as precise as solving the full set of equations numerically, it offers a number of important insights and gets around the requirement of knowing the detailed chemical kinetics.

The model considers the flow generated by the motion of a constant velocity shock wave in planar, cylindrical and spherical geometries. As this shock wave passes through a gas mixture, the gas temperature and pressure increases. Due to this increase in temperature and pressure, ignition can occur in the shock heated gas mixture after the elapse of a certain time and this may lead to a detonation.

A constant velocity shock wave can be formed in each of the three geometries by the motion of a constant velocity piston[10,11]. Furthermore, it has been shown[11] that a pressure and velocity field identical to that ahead of a constant velocity piston can be generated by appropriate energy addition. In Appendix A we have derived expressions for the energy and the power which must be delivered by a source to generate a constant velocity piston in the three geometries. The source power required is given by

$$P_s(t) = \frac{\gamma}{(\gamma-1)} C_\alpha p_p u_p^\alpha t^{\alpha-1} \quad , \tag{1}$$

where $C_\alpha = 1,\ 2\pi,\ 4\pi$ for $\alpha = 1,2,3$ corresponding to the planar, cylindrical and spherical geometries respectively; p_p and u_p are the pressure and velocity at the piston surface and t is the duration of energy deposition. The energy deposited is given by the time integral of the power, that is

$$E_s(t) = \frac{\gamma}{(\gamma-1)} \frac{C_\alpha}{\alpha} p_p u_p^\alpha t^\alpha \quad . \tag{2}$$

From the above equations we note that a planar energy source with a constant rate of energy deposition can generate a constant velocity piston in a planar geometry. An example of such an energy source is the high pressure driver in a uniform shock tube. However for a constant velocity piston in a cylindrical geometry, we need a line source with a rate of energy deposition proportional to time, and in a spherical geometry we need a point source with an energy deposition rate proportional to the second power of the time.

Equations (1) and (2) give the source power and the source energy required to generate a constant velocity piston in the three geometries. As shown later (in Appendix B), if the piston velocity is steady, a constant velocity shock wave could be generated ahead of it. If the piston velocity is reduced (by altering the energy deposition rate), rarefaction waves will be generated ahead of it and these, on catching up with the shock wave , will reduce the shock velocity. However if the shock has been in motion for a sufficiently long time, chemical reactions would begin in the shock heated gas mixture. Then, even if the piston decelerates and produces rarefaction waves, these will have very little effect on the motion of the shock. In this case we could have a detonation.

Let us call the minimum time of shock travel required to initiate a detonation t_{cr}. Using this in Eqs. (1) and (2), we have

$$(E_s)_{cr} = \frac{\gamma}{(\gamma-1)} \frac{C_\alpha}{\alpha} p_p u_p^\alpha t_{cr}^\alpha \quad . \tag{3}$$

and

$$(P_s)_{cr} = \frac{\gamma}{(\gamma-1)} C_\alpha p_p u_p^\alpha t_{cr}^{\alpha-1} \quad . \tag{4}$$

In the planar case, the pressure p_p and fluid velocity u_p at the piston surface are the same as those just behind the shock. However, in the cylindrical and spherical cases, the flow field between the shock and the piston surface is nonuniform and can be obtained by solving the governing partial differential equations. However, the solution procedure is considerably simplified if we seek a similarity solution. The details of this solution procedure are given in Appendix B.

In order to determine the power-energy relation using Eqs. (3,4) we also need to know t_{cr}. This time must at least be equal to the time at which ignition first occurs in the flow field[9]. As noted by Urtiew and Oppenheim,[12] ignition usually occurs first at the contact surface (i.e., at the piston surface here) since the temperature and pressure is highest at this location. So a first estimate of the time t_{cr} would be the induction delay time corresponding to the conditions at the piston surface.

III. RESULTS AND DISCUSSION

We have used the model described above to determine the power-energy relations for the initiation of planar, cylindrical, and spherical detonations in a stoichiometric oxy-acetylene mixture. The initial temperature and pressure of the mixture were taken to be 300 K and 100 torr (0.1316 atm) to correspond to the initial conditions in the experiments of Knystautas and Lee[6]. As a first approximation, the time duration necessary for successful initiation was assumed to be equal to the chemical induction time of the mixture corresponding to the conditions at the piston surface.

The critical source power given by Eq. (4) is time dependent for the cylindrical and spherical cases. In order to relate the critical source energy to a critical source power, we need to define an average or "effective" power. Following Abouseif and Toong[9], we define an average critical source power as

$$(P_s)_{av} = \frac{(E_s)_{cr}}{t_{cr}}. \qquad (5)$$

This power also corresponds to the critical peak averaged power of the source as defined by Knystautas and Lee[6]. For the discussion below, we have used the terms power and energy to refer to the average critical source power (Eq. (5)) and the critical source energy (Eq. (3)).

A. Cylindrical Detonations in an Acetylene-Oxygen-Nitrogen Mixture

We have determined the power-energy relation for the initiation of cylindrical detonations using Eqs. (3) and (5). The induction time data used were those obtained by Edwards et al.[13] for an acetylene-oxygen-nitrogen (2:5:4) mixture and are given by:

$$\text{Log}\,(\tau[O_2]) = -9.41\ (\pm\ 0.2) + \frac{71.35\ (\pm\ 3.34)}{19.14\ T} \qquad (6)$$

where τ is the induction time in seconds, $[O_2]$ is the concentration in mol/liter, and T is the temperature in thousands of degrees K. Three different power-energy relations obtained from the theoretical model are shown in Figure 1. Curve A was obtained by using the smallest value of the induction time given by Eq. (6), that is, by choosing the negative signs. Curve B was obtained by using the mean values and curve C by using the largest value of the induction time (by choosing the positive signs). The arrows on curve C indicate the direction of increasing Mach number. First, we note that each curve has a minimum power and a minimum energy. We also observe that as the Mach number decreases below the Mach number corresponding to the minimum power, both the average source power and the source energy increase. However, when the Mach number increases above the Mach number corresponding to the minimum power, the energy first decreases to the minimum energy and then increases again. All three curves exhibit these same qualitative trends.

The shape of these curves can be explained in the following manner. As the Mach number of the shock wave decreases, the pressure and the temperature behind it decrease. This decrease also results in a decrease of the pressure and velocity at the piston surface. This would tend to decrease both the power and the energy since, as seen in Eqs. (1,2),

$$P \sim p_p u_p^2 t \tag{7}$$

$$E \sim p_p u_p^2 t^2 \quad . \tag{8}$$

This tendency is, however, opposed by the tendency of the induction time to increase with decreases in the pressure and the temperature. For low Mach numbers, (i.e., low temperatures behind the shock) a small decrease in the Mach number of the shock wave leads to a large increase in the induction

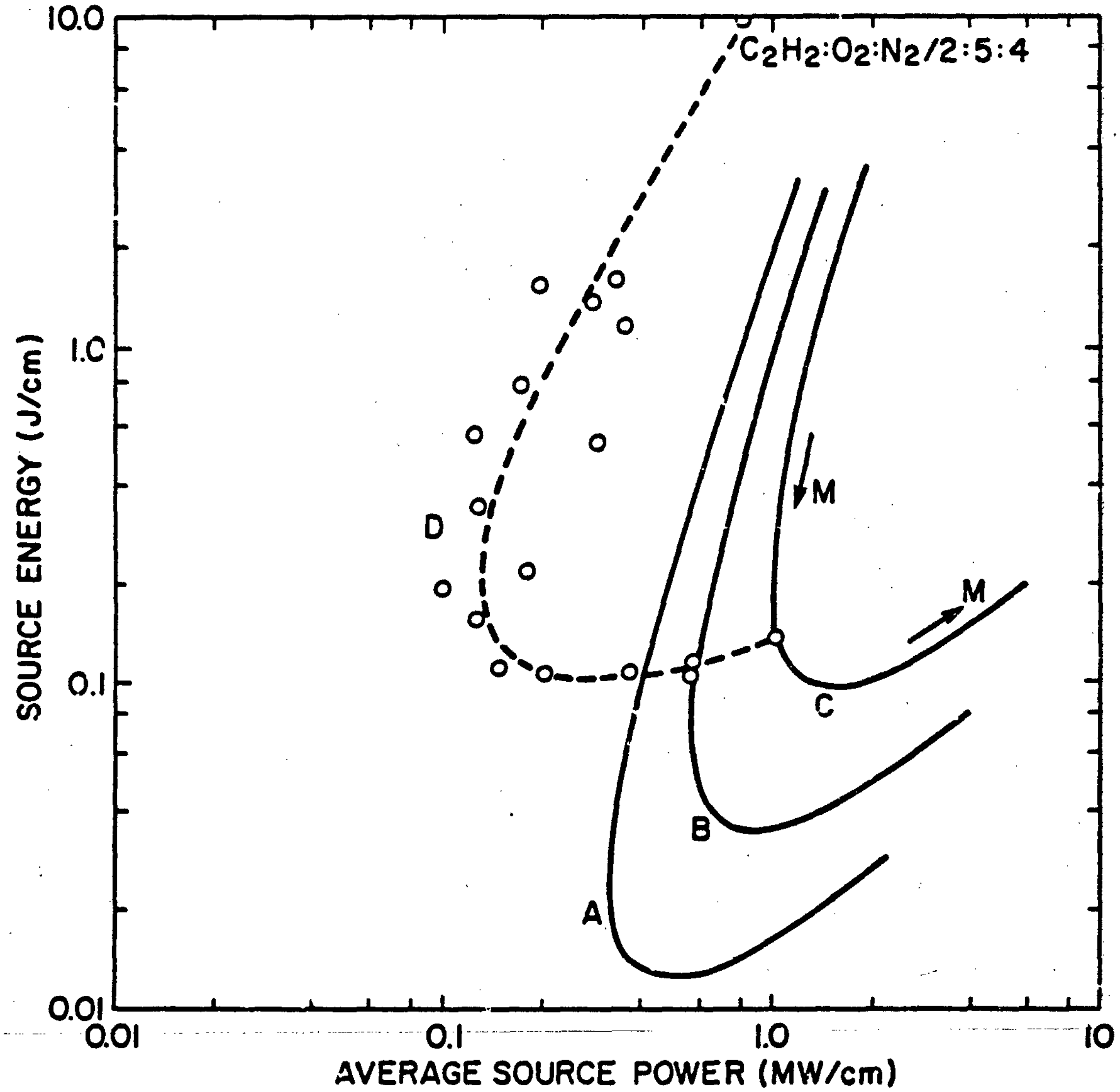

Figure 1. Power-energy relations for the initiation of cylindrical detonations in an acetylene-oxygen-nitrogen mixture (2:5:4) at 0.1316 atm and 300K. The data for curve D was obtained from spark ignition experiments [6]. Curves A, B, and C are explained in the text. The arrows on Curve C indicate the direction of increasing Mach number.

time. The shape of the curves in Figure 1 implies that this increase in induction time is more than sufficient to compensate for the decrease in the pressure and the velocity for Mach numbers below that corresponding to the minimum power. Therefore both the power and the energy increase with decreasing Mach number. Since the energy is proportional to the product of the power and the induction time (Eqs. (7,8)), the energy increases faster with induction time than the power does. As the Mach number increases above that corresponding to the minimum power, the increase in the pressure and velocity is larger than the decrease in the induction time. Therefore the power increases. However, for a certin range of Mach numbers, the increase in the pressure and velocity is not sufficient to compensate for the decrease in the square of the induction time. Therefore the energy decreases until it attains a minimum value, even though the power increases. Finally, for Mach numbers above that corresponding to the minimum energy, the increase in the pressure and velocity are easily able to overcome the decrease in the induction time with increasing Mach number and both the power and the energy increase. This occurs because the rate of decrease of the induction time with temperature is small for high temperatures (i.e., high Mach numbers) according to Eq. (6).

The power-energy curve obtained using data from the spark ignition experiments[6] of Knystautas and Lee has also been included in Figure 1 as curve D. The data for curve D is the same as that used by Abouseif and Toong[9] for their Figure [1], and was originally presented in Figure [4] of Knystautas and Lee[6]. Curve D exhibits the same qualitative trends as those of the theoretical curves discussed above. However, we observe that the values of the minimum power and the minimum energy from the four curves are very different from each other. The differences in the values of these parameters from the three "theoretical" curves (A,B, and C) indicate that the experimental uncertainties in the values of the induction times used have a significant effect on the value of the minimum power and the minimum energy. The minimum power varies from about 0.3 MW/cm to about 1 MW/cm and the minimum energy varies from about 0.012 J/cm to about 0.1 J/cm. The experimentally determined minimum power (from curve D) is about 0.13 MW/cm, which is lower than the calculated values, and the minimum energy is about 0.1 J/cm, which is at the top of the range of calculated values.

The quantitative differences between the experimental and theoretical values could be due to a variety of factors, a few of which we now discuss. As observed from curves A, B, and C, uncertainties in the induction time data can have a significant effect on the values of the minimum power and the minimum energy. Expressions such as Eq. (6) for the induction time are obtained by fitting to a limited range of experimental data. However, here we have used Eq. (6) for a range of temperatures and pressures far greater than that over which it was determined. The Mach numbers and the corresponding temperatures and pressures at the shock and the piston surface, along with the induction time used for obtaining curve B, are given in Table I. We see that for Mach numbers greater than about 14, the temperatures and pressures are so high that the entrapolated induction time is of questionable validity. However, for obtaining the theoretical results, we had assumed a constant value of 1.2 for γ, the ratio of specific heats. We see from Table I that for high Mach numbers, the γ of the shocked gas could be very different from that ahead of the shock wave because of the large temperature differences. Using an incorrect value for γ could also

TABLE I

Parameters at the Piston Surface for Shocks of Different Strengths

M	P_s(atm)	T_s(K)	p_p(atm)	T_p(K)	τ_p(μsec)
4.0	2.285	769.5	2.378	774.6	1485.3
5.0	3.577	1037.9	3.701	1043.8	73.823
6.0	5.156	1365.4	5.320	1372.6	9.4207
7.0	7.023	1752.4	7.232	1761.0	2.2381
8.0	9.176	2198.8	9.439	2209.2	0.8003
9.0	11.616	2704.6	11.939	2717.0	0.37639
10.0	14.344	3270.0	14.736	3284.7	0.21357
12.0	20.661	4579.2	21.209	4599.2	0.098452
14.0	28.126	6126.3	28.859	6152.6	0.060420
16.0	36.740	7911.5	37.685	7945.0	0.043616
18.0	46.502	9934.6	47.687	9976.4	0.034733
20.0	57.413	12195.8	58.870	12246.8	0.029447

Note: A constant γ of 1.2 has been assumed for obtaining the above results.

explain some of the quantitative differences between the experimental and theoretical results.

B. Effect of γ on Power-Energy Relations

We have repeated the power-energy calculations using different but constant values for γ on both sides of the shock wave and the results are shown in Figure 2. We observe that γ does indeed have a significant effect on the minimum power and the minimum energy. When γ is changed from 1.1 to 1.4, the minimum source power decreases from 2.0 MW/cm to 0.18 MW/cm and the minimum energy decreases from 0.065 to about 0.02 J/cm. The Mach number at which the shock must travel to attain the minimum power is also very different, as seen in Figure 3 where the average source power is shown as a function of Mach number for three values of γ. Changing γ from 1.4 to 1.1 doubles the Mach number corresponding to the minimum power from 8 to 16. The effect of γ on the power-energy relation arises partly from the factor $(\gamma/\gamma\text{-}1)$ in Eqs. (3) and (4) and partly from the fact that the temperature behind a shock of given Mach number is very different for different γ's.

The effect of the factor $(\gamma/\gamma\text{-}1)$ is to change quantitatively the values of the source power and the source energy corresponding to the shock of a given Mach number and is the same for all Mach numbers. The changes in the temperature behind a shock wave due to assumed differences in γ is, however, a function of the shock Mach number. Let us consider a shock wave of the Mach number 10. In Table II we have given the pressure ratio, the temperature ratio and the temperatures across this shock wave for different values of γ. We have also included the case where γ is different across the shock wave as case 3. For obtaining case 3, Eqs. (C7-C13) from Appendix C

TABLE II

Effect of the Ratio of Specific Heats

CASE	γ_o	γ_s	p_s/p_o	T_s/T_o	T_o	T_s
1	1.2	1.2	109.000	10.900	300	3270.0
2	1.3	1.3	112.913	15.710	300	4712.89
3	1.3	1.2	118.426	11.454	300	3436.26

Note: The conditions ahead of the shock wave are denoted by "o" and those behind by "s".

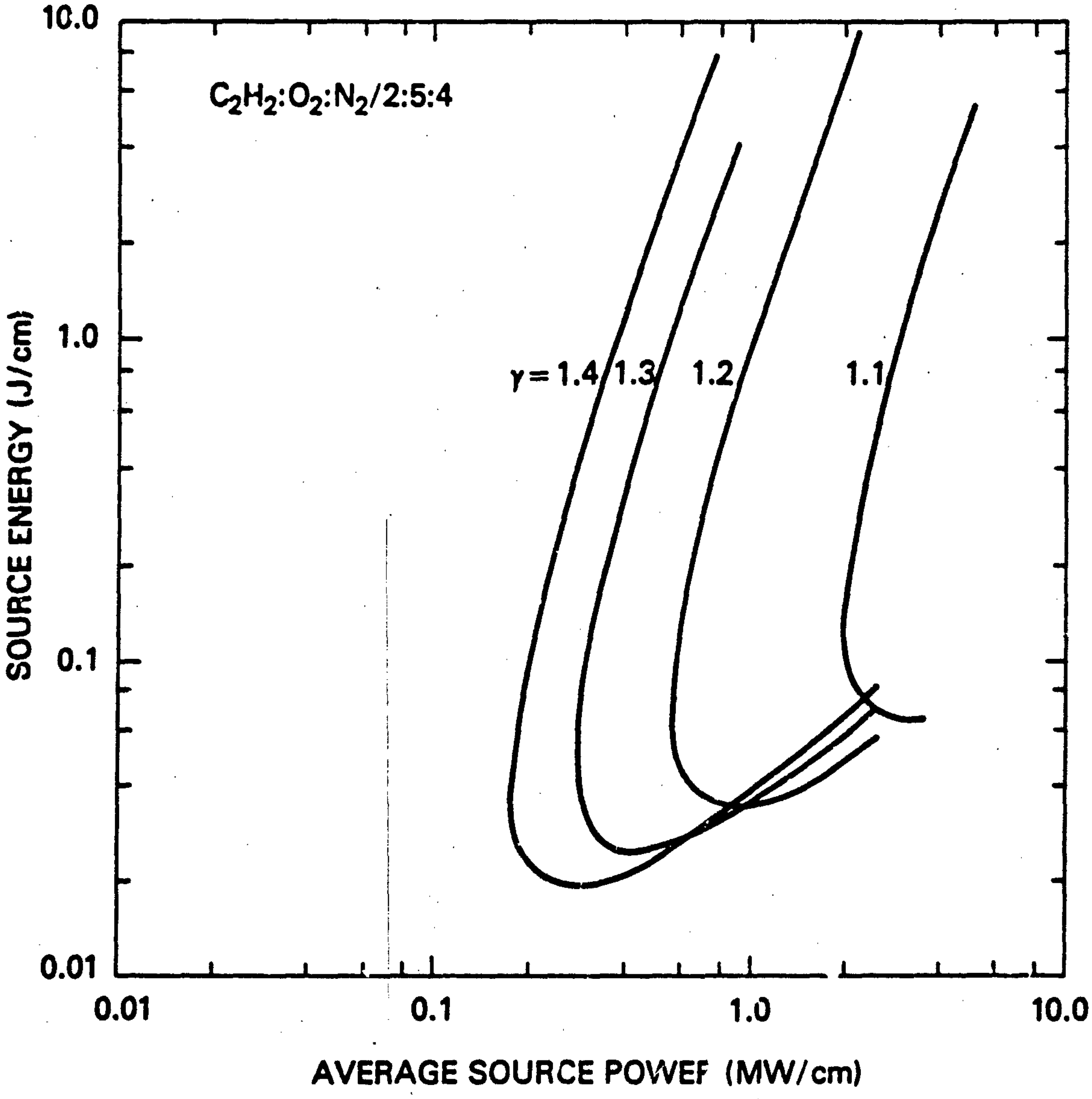

Figure 2. Effect of γ on the power-energy relations for the initiation of cylindrical detonations in an acetylene-oxygen-nitrogen mixture.

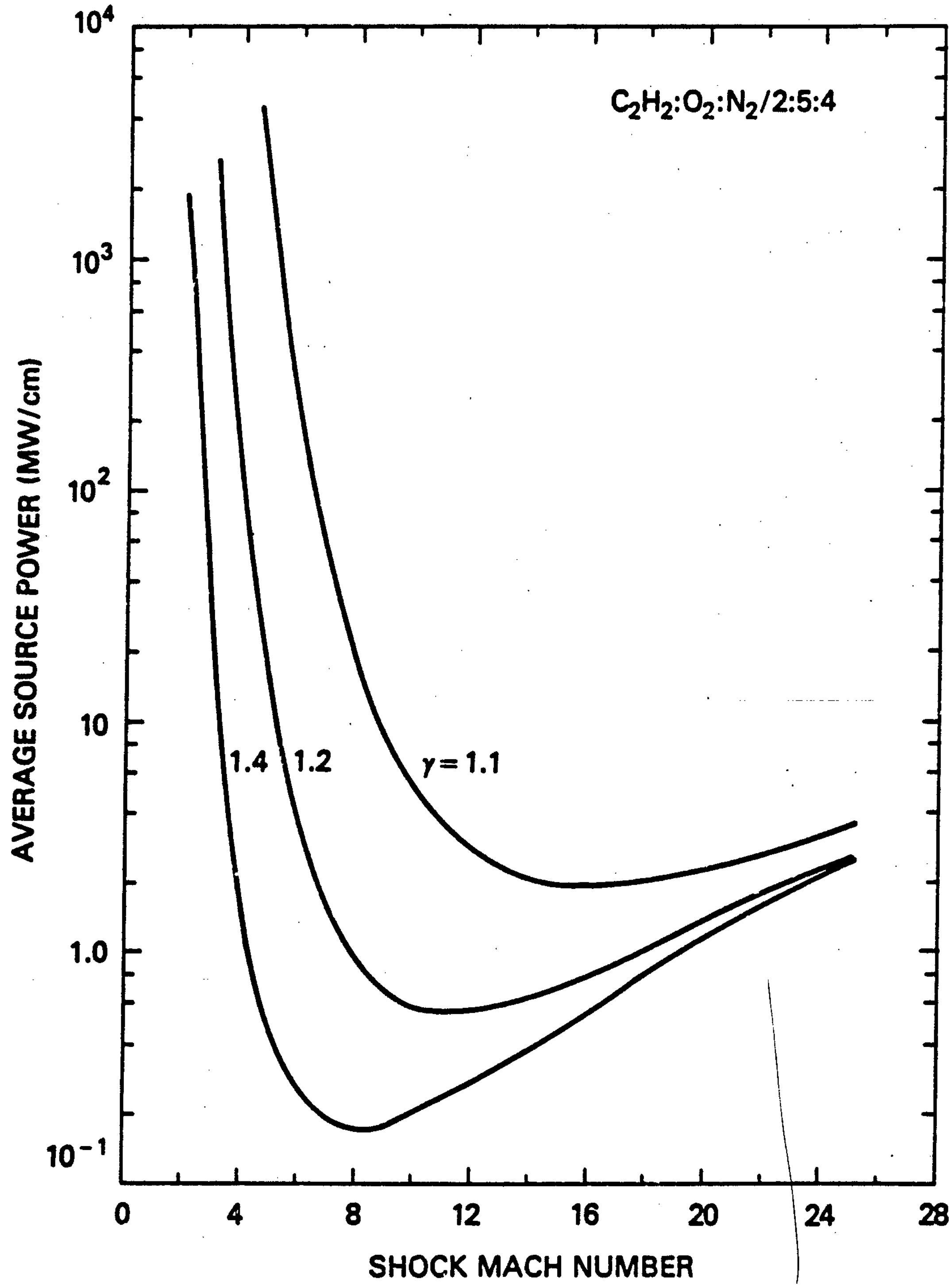

Figure 3. The average source power as a function of the shock Mach number for constant γ's across the shock wave.

were used. We see that the temperature behind the shock wave is significantly lower than that for case 2. Case 3 is a more realistic case than case 2, since γ is generally lower behind the shock. However, the appropriate γ for conditions behind the shock wave is different for different Mach numbers, since the temperatures are different. Thus a better approach is first to guess a γ for each Mach number and use it to calculate the temperature behind the shock. This new temperature implies a new γ, as discussed in Appendix C. Using this new γ in the modified shock relations (Eqs. (C7–C13)), we get a new temperature. This iterative procedure can be continued till convergence is achieved.

The power-energy calculations were repeated using the correct value for γ, that is, for each Mach number including the effect of temperature on γ. In Figures 4 and 5, the average source power and the source energy have been shown as functions of the Mach number for three different conditions (A, B, and C). Curves A and C were obtained assuming γ constant and have already been discussed. Curve B is obtained using the variable γ. For low Mach numbers, curve B lies close to curve A and for very high Mach numbers it tends towards curve C. This is not surprising since for the acetylene-oxygen-nitrogen mixture being studied here, γ varies from 1.31 to 1.16 when the Mach number changes from 2 to 24. From curve B in Figures 4 and 5 we also note that the minimum power and the minimum energy conditions occur at Mach number of 10.0 and 15.5 respectively. The power-energy curve obtained with the variable γ is shown as curve B in Figure 6 where we have also shown three other curves obtained assuming constant γ. We note that curve B lies predominantly between the curves with γ of 1.1 and 1.3 and is very similar to the curve with γ of 1.2.

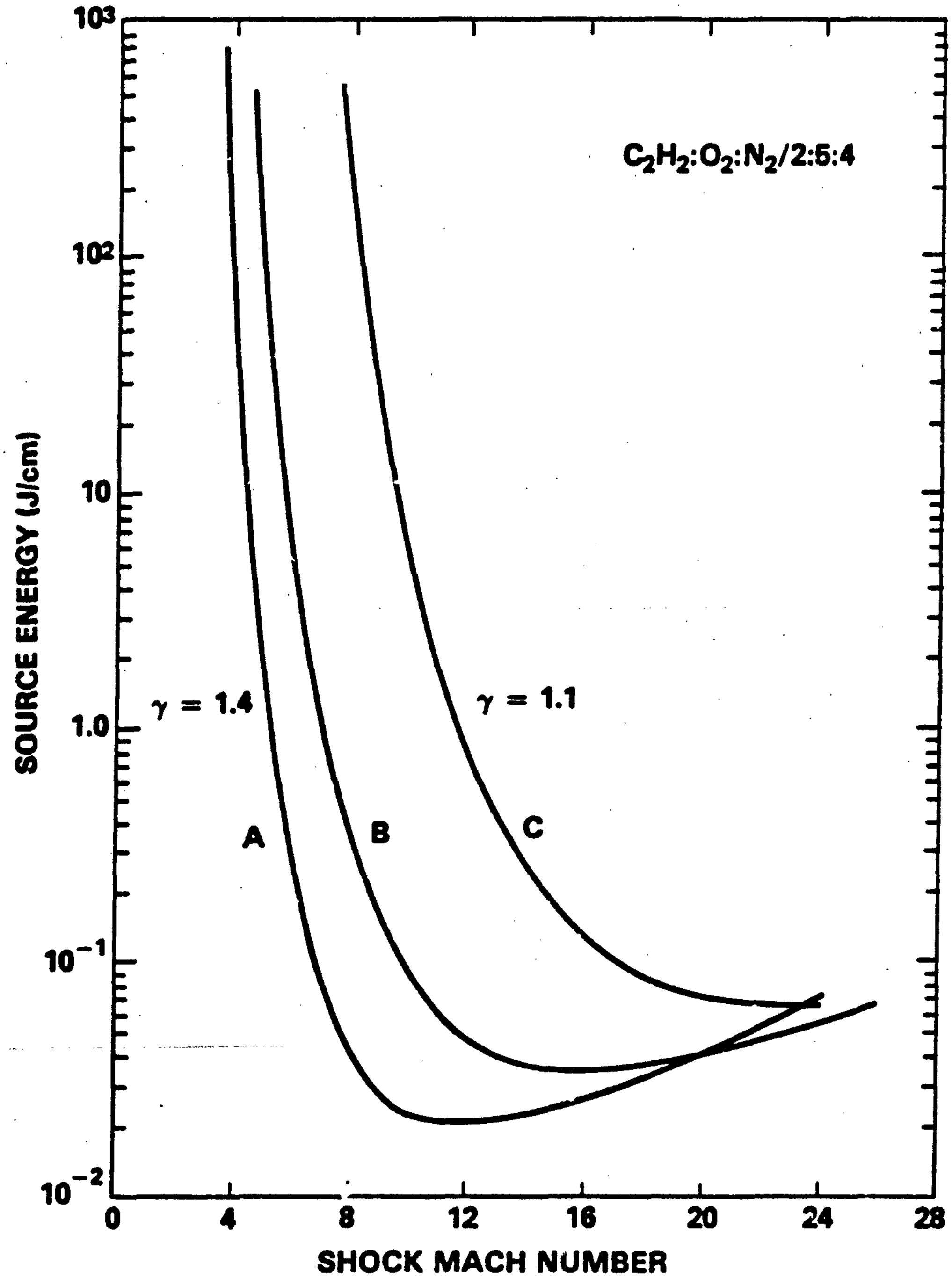

Figure 4. The source energy as a function of the shock Mach number. Curves A and C were obtained assuming γ to be constant across the shock wave. Curve B was obtained assuming γ to be variable as explained in the text.

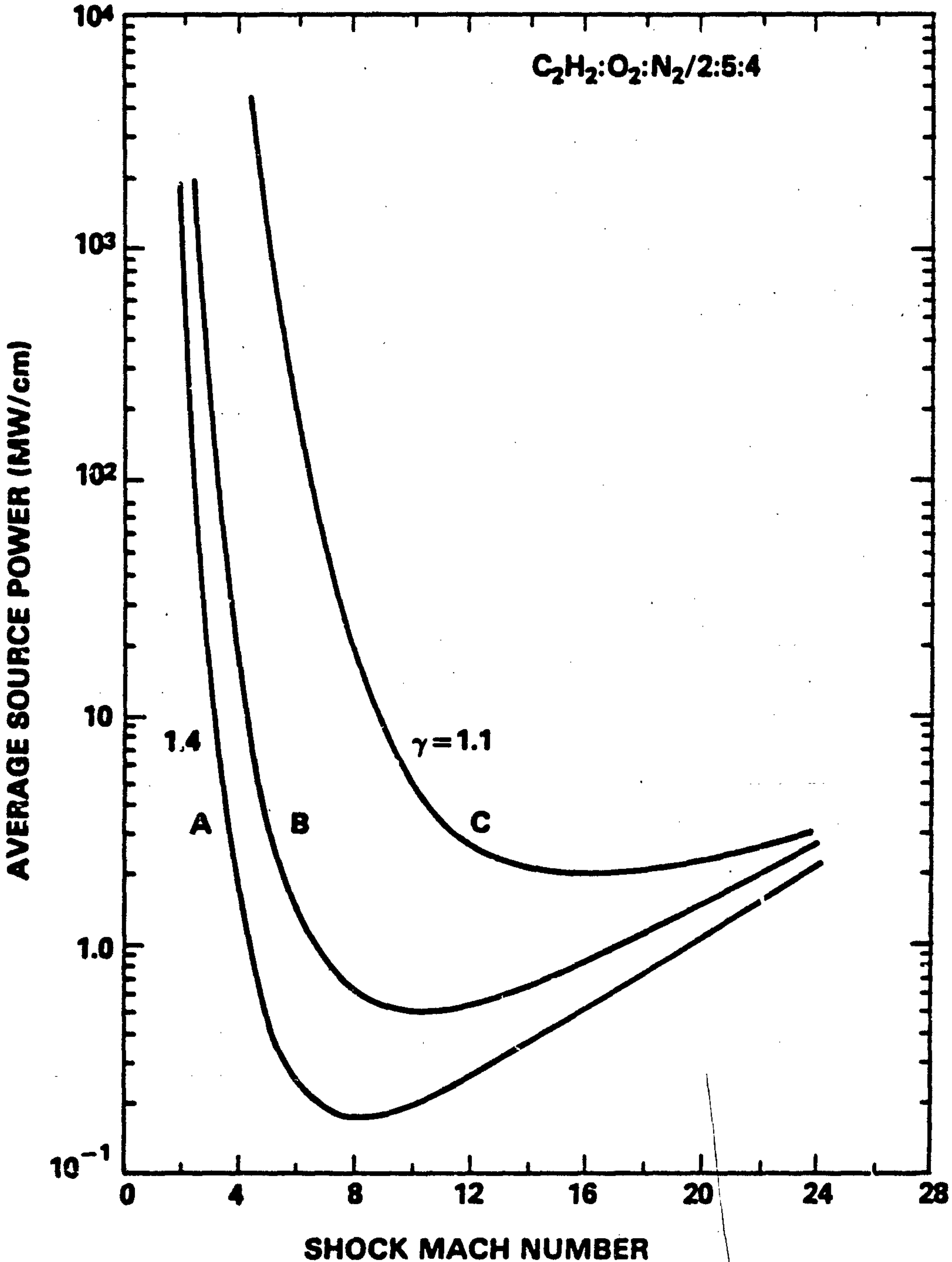

Figure 5. The average source power as a function of the shock Mach number. Curves A and C were obtained assuming γ to be constant across the shock wave. Curve B was obtained assuming γ to be variable as explained in the text.

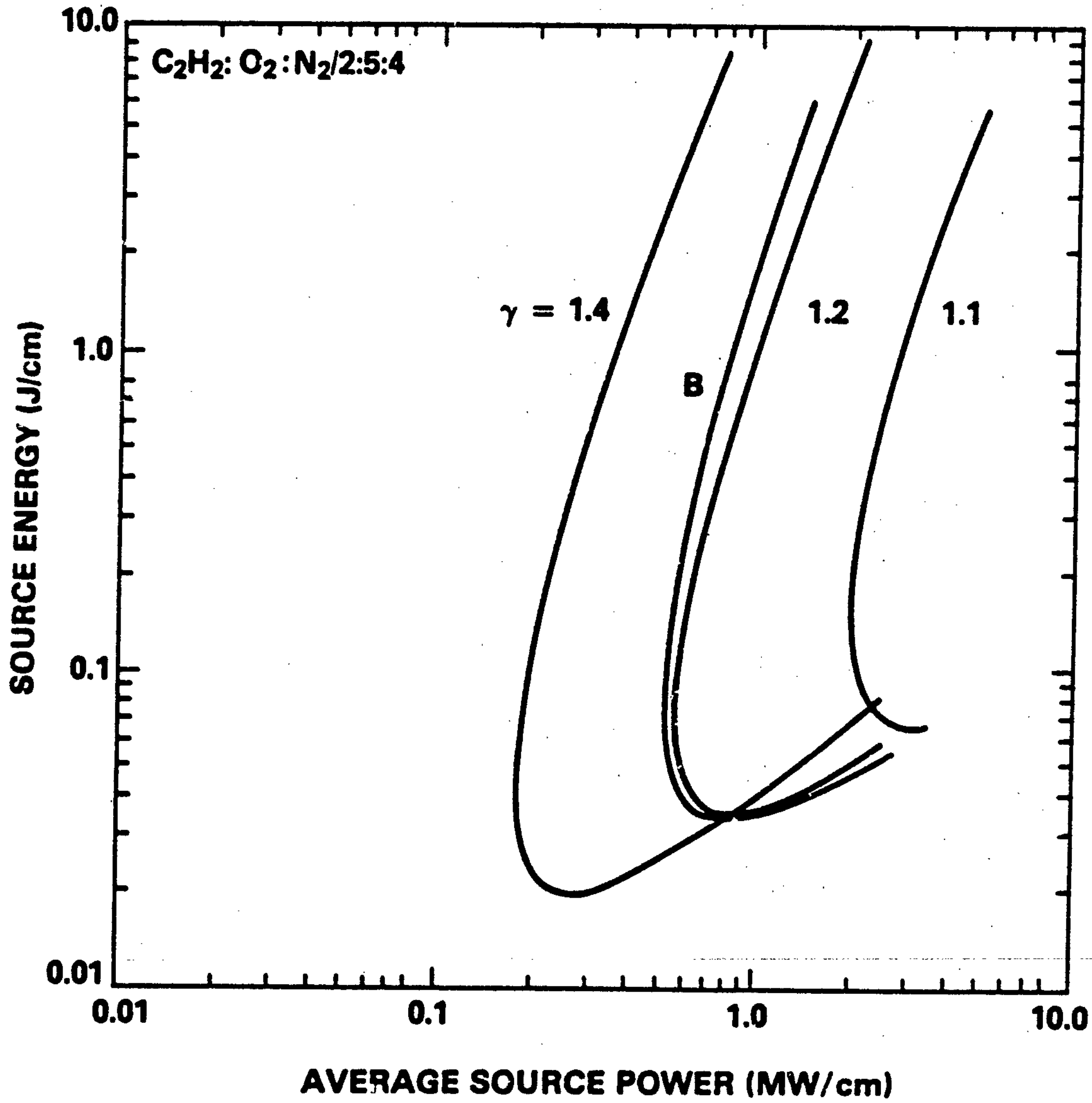

Figure 6. Effect of variable γ on the power-energy relations for the initiation of cylindrical detonations in an acetylene-oxygen-nitrogen mixture.

From the above discussion it is clear that the effect of using the correct γ is mainly to alter the Mach number corresponding to the minimum power and the minimum energy condition. However, the calculated values of the minimum power and the minimum energy are still different from those obtained experimentally. Therefore we examine another possible reason for the differences between the experimental and the theoretical values: the uncertainty in the appropriate time to be used for t_{cr} in Eqs. (3) and (5).

C. Critical Time for Energy Deposition

As a first approximation, we assume that energy must be deposited until ignition occurs at some point in the flow field between the shock and the piston surface. Since, in general, the temperature and pressure is highest at the piston surface, we used the chemical induction time corresponding to these conditions as the appropriate time for energy deposition. However, when there is fluid motion, ignition can occur before the time corresponding to the constant volume, homogeneous chemical induction time. For example, for a certain range of temperatures and pressures, oxy-hydrogen mixtures with small perturbations could have significantly reduced ignition times. The specific effect of this phenomenon on the power-energy relations will be reported in a subsequent paper. In gas mixtures which are not particularly sensitive to perturbations, the shortest induction time in the shocked region seems to be the necessary condition for the initiation of detonations. However, we need to consider whether this is a sufficient condition also.

Shock tube simulations[14] have indicated that the time at which a detonation wave is first observed is only very slightly longer than the time at which ignition first occurs. That is, the time between ignition and the formation of a detonation wave is small when compared to the induction time. This is not surprising when we consider the fact that for many reactive systems, the reaction time is very small compared to the induction time. The results of Abouseif and Toong on the initiation of planar detonations[9] also supports this observation. However we have not studied the effect of geometry on the time between ignition and detonation. It could very well be that due to the volume change in spherical and cylindrical geometries, this time is significant when compared to the induction time. This needs to be studied before one can confidently use the induction time as the appropriate time for t_{cr}.

We have compared the results from the theoretical model for the case of cylindrical detonations with the experimental results of Knystautas and Lee[6] because in both cases the amount of energy deposited was proportional to the second power of the time. However, it is important to note that in the theoretical model we have considered only constant velocity shock waves and it was this that made it possible to assign a single induction time to each shock wave. If the velocity of the shock wave is not constant, it is not possible to assign a single induction time to it since the flow field behind the shock wave would be time-dependent. Thus, shock waves of different time histories can deposit the same amount of energy but at different average source powers. This could be an imporant factor in the quantative differences between the experimental and theoretical values.

D. Initiation of Planar Detonations

The derived power-energy relation for the initiation of planar detonations in the same oxy-acetylene mixture is shown in Figure 7. In this

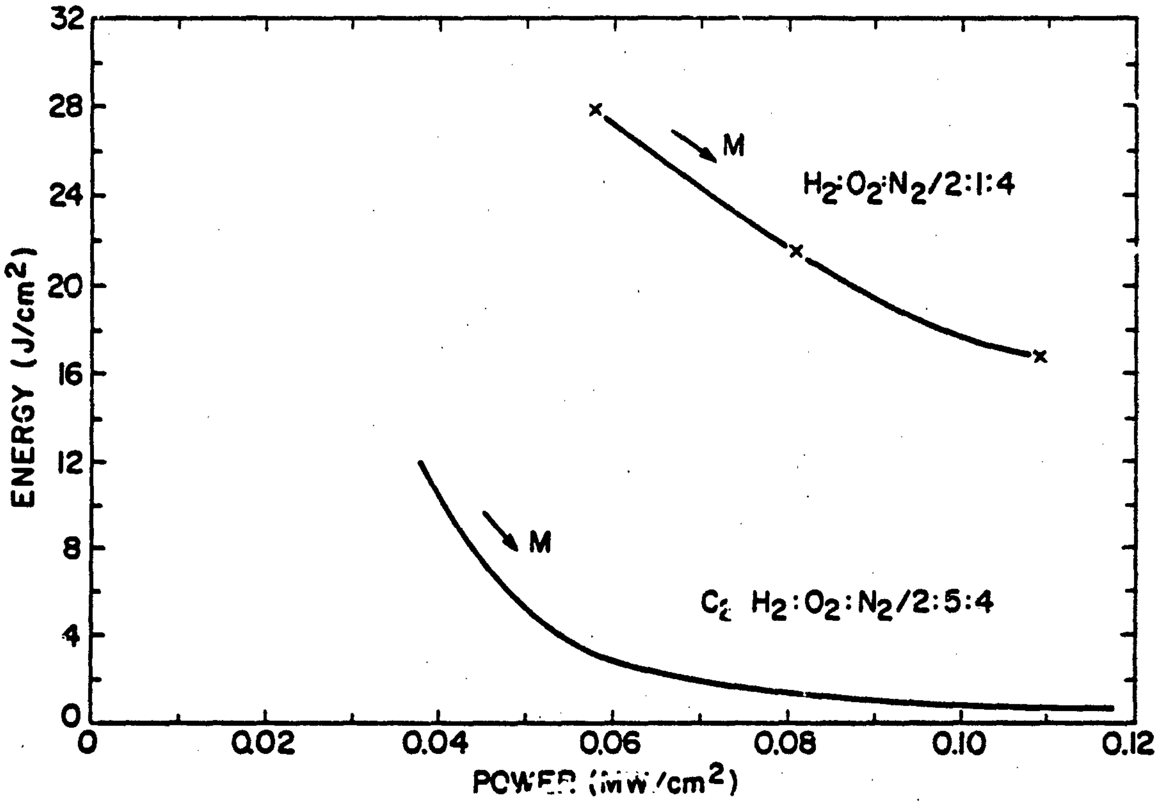

Figure 7. Power-energy relations for the initiation of planar detonations. The x's are data obtained from shock tube experiments [7].

figure, we also show the shock tube data of Dabora[7] on the direct initiation of detonations in a stoichiometric hydrogen-air mixture. The point to notice is that both curves exhibit the same qualitative behavior. Unlike the cylindrical case, each value of the power corresponds to an unique value of energy. The direction of increasing shock strength (as determined by the Mach number) is also shown in Figure 7. In the planar case, we see that as the Mach number decreases the power always decreases. As noted earlier in the cylindrical case, as the Mach number decreases, the power decreases only up to the minimum power. Then the power increases with a decrease in the Mach number of the shock wave. Therefore, the qualitative difference in the experimental data of Knystautas and Lee (shown in Figure 1) and Dabora (shown in Figure 7) are due to the difference in the geometry of the two experiments.

We also observe in Figure 7 that as the Mach number decreases, we need more and more energy to initiate a detonation. The trend of the curves indicates that there is a minimum Mach number below which a detonation will not occur (i.e., would require an infinite amount of energy). The value of the power corresponding to this minimum Mach number is the minimum power. This agrees with the observation made by Knystautas and Lee[6] that the requirement for a minimum value of the source power indicates that the source must be capable of generating a shock wave of a certain minimum Mach number. However, we observe from Figure 1 (see also Figures 3 and 5) that for the case of cylindrical detonations, the minimum power does not correspond to the shock wave of minimum Mach number. In the cylindrical case, it is possible to initiate a detonation with a shock wave of lower Mach number than that corresponding to the minimum power. Such a shock will have to be maintained for a longer time than the shock corresponding to the minimum power and hence will require a larger amount of energy.

E. Initiation of Spherical Detonations

The power-energy curve for the initiation of spherical detonations is similar to the curve for the cylindrical case. However, for the case of spherical detonations, the power is

$$P \sim \rho_p u_p^3 t^2, \tag{9}$$

but the energy is still

$$E \sim P\ t. \tag{10}$$

Since the power and energy are proportional to higher powers of the time, t uncertainties in t will have a greater effect on the value of the minimum power and the minimum energy. Further work is being carried out currently to study the initiation of spherical detonations in hydrogen-air mixtures and to compare this to experimental data.

IV. SUMMARY AND CONCLUSIONS

In this paper we have used a theoretical model to determine the relation between the power and the energy required for the initiation of planar, cylindrical and spherical detonations in a gas mixture. The results discussed above show that though the simple theoretical model has significant limitations, it can still be used to explain the qualitative differences in the power-energy relations obtained from different experimental arrangements. Another result from the model is that the minimum power requirement corresponds to a shock of minimum Mach number only in the case of planar detonations.

The results from the model on the initiation of cylindrical detonations in an acetylene-oxygen-nitrogen mixture qualitatively agree with experimental data. Some of the reasons for the quantitative differences have been examined. One of the important parameters in the model is the time required for deposition of the critical energy required for the initiation of detonations. This time is related to the induction time and the results presented above show that uncertainties in the induction time data used can have a significant effect on the power-energy relations. The results also indicate that further work needs to be done to determine the effect of the geometry on the time for critical energy deposition.

The quantitative differences between the experimental and theoretical results may also arise because of the model assumption that the velocity of the shock wave is constant. This may not be so in the experiments. Furthermore, the model considers only the minimum power and energy required to initiate a detonation wave. We have not examined whether this would result in a self-sustained, propagating detonation wave. Detonation propagation is characterized by complicated interactions among incident shock waves, transverse waves and Mach stems which form detonation cells. These must be described by multidimensional theories and simulations. The results from such studies need to be considered to extend the work presented here to the study of self-sustained detonation waves.

One application of the model presented here is to determine the relative tendency of different explosives to detonate, since the limitations of the model would then be less critical. This would be particularly useful for studying the effect of additives on the detonability of condensed phase explosives. Further work is being carried out to modify the model for such applications.

Appendix A

Source Power and Energy Required to Generate a Constant Velocity Piston

Here we derive the power and energy required by a source to generate a constant velocity piston in planar, cylindrical and spherical geometries. Let us first calculate the work done by a constant velocity piston moving from time t_o to time t in a gas mixture. If the effects of viscosity, heat conduction and chemical reaction are negligible during the time internal $(t-t_o)$, the pressure ahead of the constant velocity piston would also be constant. Then the work done by the piston on the gas mixture is given by

$$w = \int_{v_o}^{v} p_p \, dv = p_p \, (v - v_o) \qquad \text{(A1)}$$

where v_o and v are the volumes at time t_o and t, repectively. The volume change $(v - v_o)$ depends on the geometry of the system. In planar geometry, the volume swept out by the piston is

$$v - v_o = A(r - r_o) \quad , \qquad \text{(A2)}$$

where r_o is the position of the piston at time t_o and A is the cross sectional area of the planar piston. In cylindrical geometry,

$$v - v_o = \ell \, (\pi \, r^2 - \pi \, r_o^2) \quad , \qquad \text{(A3)}$$

where ℓ is the characteristic linear dimension of the system and in a spherical geometry,

$$v - v_o = \frac{4}{3} \pi \, r^3 - \frac{4}{3} \pi \, r_o^3 \quad . \qquad \text{(A4)}$$

The position of the constant velocity piston at time t is given by

$$r = r_o + u_p (t - t_o) \quad , \tag{A5}$$

where u_p is the velocity of the piston. Without loss of generality we can assume that $r_o = 0$ at time $t_o = 0$. Using Eq. (A5) in Eqs. (A2), (A3) and (A4), we have

$$v - v_o = \frac{B_\alpha}{\alpha} u_p^{\alpha} t^{\alpha} \quad , \tag{A6}$$

where $B_\alpha = A$, $2\pi\ell$, and 4π for $\alpha = 1$, 2, and 3 corresponding to the planar, cylindrical and spherical geometries respectively.

Substituting Eq. (A6) into Eq. (A1) we have

$$w = p_p \frac{B_\alpha}{\alpha} u_p^{\alpha} t^{\alpha} \quad . \tag{A7}$$

Defining

$$
\begin{aligned}
w_p &= \frac{w}{A} \quad \text{for } \alpha = 1 \quad , \\
&= \frac{w}{\ell} \quad \text{for } \alpha = 2 \quad , \text{ and} \\
&= w \quad \text{for } \alpha = 3 \quad ,
\end{aligned} \tag{A8}
$$

we have

$$w_p = \frac{C_\alpha}{\alpha} p_p u_p^{\alpha} t^{\alpha} \quad . \tag{A9}$$

It is important to note that the above expression for w_p gives the work done by the piston, per unit area in planar geometry and per unit length in cylindrical geometry.

In order to obtain the above amount of work w_p, we will need a source which can generate and maintain such a constant velocity piston. It has been shown that a pressure and velocity field identical to that ahead of such a piston can be generated by appropriate heat addition. In order to demonstrate this, consider heat addition to a closed system of arbitrary volume v_o. For such a system with no heat losses to the surroundings, the first law of thermodynamics states that the change in the internal energy of the system is

$$dE_{int} = dq + dw \tag{A10}$$

where dq is the amount of heat energy deposited and dw is the work done by the system. Let us assume that heat energy is added to the system to take it from the volume v_o to the volume v at a constant pressure, p. Then, the change in the internal energy of the system (assuming a mixture of perfect gases) is given by

$$dE_{int} = \frac{pv}{\gamma-1} - \frac{pv_o}{\gamma-1} = \frac{p}{\gamma-1}(v-v_o). \tag{A11}$$

The work done by the system in going from v_o to v at the constant pressure p is

$$dw = -\int_{v_o}^{v} pdv = -p(v-v_o) \ . \tag{A12}$$

Substituting Eqs. (A11) and (A12) in Eq. (A10), we find that the amount of heat energy which has to be deposited to create the required change in the system is

$$\begin{aligned} E_{dep} &= \frac{p}{\gamma-1}(v-v_o) + p(v-v_o) \\ &= \frac{\gamma}{\gamma-1} p(v-v_o) \end{aligned}$$

$$= \left(\frac{\gamma}{\gamma-1}\right) W. \tag{A13}$$

Substituting Eq. (A9) in Eq. (A13) we have the source energy required to create a constant velocity piston in the three geometries,

$$E_s(t) = \frac{\gamma}{\gamma-1} \frac{C_\alpha}{\alpha} p_p \; u_p^\alpha + t^\alpha \quad . \tag{A14}$$

The power, or the rate at which energy is deposited, is given by

$$P_s(t) = \left.\frac{dE_s}{dt}\right|_t$$

$$= \frac{\gamma}{\gamma-1} C_\alpha \; p_p \; u_p^\alpha \; t^{\alpha-1}. \tag{A15}$$

Appendix B

Flow Field between the Piston Surface and Shock Wave

In the planar case, the pressure and fluid velocity at the piston surface are the same as those just behind the shock. However, in the cylindrical and spherical cases, the flow field between the shock and the piston surface is nonuniform but can be obtained by solving the following equations. For a one-dimensional flow, the equations for the conservation of mass can be written as:

$$\frac{\partial\rho}{\partial t} + u\,\frac{\partial\rho}{\partial r} + \rho\left[\frac{\partial u}{\partial r} + (\alpha-1)\,\frac{u}{r}\right] = 0, \tag{B1}$$

and for conservation of momentum as:

$$\frac{\partial u}{\partial t} + u\,\frac{\partial u}{\partial r} = -\frac{1}{\rho}\,\frac{\partial p}{\partial r}, \tag{B2}$$

where α = 1, 2, and 3 for planar, cylindrical and spherical coordinates respectively. Since we are primarily concerned with the flow field before any significant reactions occur, we can assume the flow is isentropic if diffusive transport effects are negligible. For a perfect gas, the energy equation then becomes

$$\frac{dp}{d\rho} = \frac{\gamma p}{\rho}. \tag{B3}$$

We can obtain the flow field between the piston surface and the shock wave by solving the above system of partial differential equations with appropriate boundary conditions. However, the solution procedure is considerably simplified if we seek a similarity solution. Then the system of partial differential equations can be reduced to a system of coupled ordinary differential equations:

$$\frac{(u-L)}{\rho}\frac{d\rho}{dL} + \frac{du}{dL} + (\alpha-1)\frac{u}{L} = 0 \tag{B4}$$

$$(u-L)\frac{du}{dL} = -\frac{1}{\rho}\frac{dp}{dL} \tag{B5}$$

$$\frac{dp}{dL} = \frac{\gamma p}{\rho}\frac{d\rho}{dL} \quad . \tag{B6}$$

In the above system of equations, the density ρ, the velocity u and the pressure p are all functions of the similarity variable L, which is equal to the radial location r divided by the time t. For a spherical geometry (α=3), Eqs. (B4) - (B6) reduce to those formulated by Taylor[10]. These equations can be further reduced to a set of two equations in the dependent variables u and a, the sound speed, which is a function of p and ρ. For a mixture of perfect gases, using

$$a^2 = \frac{\gamma p}{\rho} \tag{B7}$$

and appropriately combining Eqs. (B4) - (B6) we have:

$$\frac{da^2}{dL} = -(\gamma-1)(u-L)\frac{du}{dL} \tag{B8}$$

and

$$\frac{du}{dL} = -(\alpha-1)\frac{u}{L}\left[1-\left(\frac{u-L}{a}\right)^2\right]^{-1} \quad . \tag{B9}$$

The boundary conditions for obtaining the flow field between the shock wave and the piston surface are: just ahead of the piston surface

$$L_p = \frac{r_p}{t} = u_p \tag{B10}$$

and just behind the shock,

$$L_s = \frac{r_s}{t} = S_u \ , \tag{B11}$$

$$a_s{}^2 = \frac{\gamma p_s}{\rho_s} \ , \tag{B12}$$

and

$$u = u_s \ . \tag{B13}$$

Normal shock relations can be used to estimate u_s, ρ_s and p_s for a shock of known velocity, S_u.

Taylor solved the equivalent of Eqs. (B8) and (B9) in spherical coordinates to obtain the properties of the airwave surrounding an expanding sphere[10]. He first assumed a piston Mach number and then numerically integrated the equations from the piston surface to different locations ahead of it. He then solved the normal shock relations for various shock strengths. When he plotted these two solutions, he fcund that there was a location in the flow field ahead of the piston which had the same physical conditions (velocity and sound speed) as that behind a shock wave of a particular Mach number. Therefore, he could uniquely relate the flow field ahead of a piston of given Mach number to that behind a particular shock wave. The existence of such a unique solution implies that a constant velocity piston will produce a constant velocity shock wave (in a spherical geometry). Since we find that such solutions exist in cylindrical geometries too, we can say that a constant velocity piston will produce a constant velocity shock wave in planar, cylindrical and spherical geometries provided we have a similarity solution.

We have adopted a different approach to solve Eqs. (B8) and (B9). For a shock of given Mach number, we determine the flow conditions behind it using the normal shock relations given in Appendix C. Knowing a_s and u_s, Eqs. (B8) and (B9) can be numerically integrated from L_s to the piston location L_p to give u_p and $a^2{}_p$. However we do not know L_p a priori. So we have to solve the equations until we find a L_p which is equal to u_p [See Eq. (B10)]. Therefore it is more convenient to rewrite Eqs. (B8) and (B9) in terms of a new dependent variable u/L. Then, we can solve the equations from u_s/L_s to 1.

Transforming Eqs. (B8) and (B9) to the new dependent variable ξ, where

$$\xi = \frac{u}{L} \tag{B14}$$

and defining

$$\eta = \frac{a^2}{L^2} \tag{B15}$$

and

$$z = \log_e L, \tag{B16}$$

we have

$$\frac{d\eta}{d\xi} = \frac{\eta[2\eta - 2(1-\xi)^2 - \xi(\alpha-1)(\alpha-1)\ (\gamma-1)\ (\xi-1)]}{\xi\ [\alpha\eta - (1-\xi)^2]} \tag{B17}$$

and

$$\frac{dz}{d\xi} = \frac{-1}{\xi}\ \frac{\eta - (1-\xi)^2}{[\alpha\eta - (1-\xi)^2]}\ . \tag{B18}$$

Eqs. (B17) and (B18) are solved along with the boundary conditions given below. Just behind the shock, that is, at

$$\xi_s = \frac{u_s}{S_u}\ , \tag{B19}$$

$$z = \log_e (S_u) \tag{B20}$$

and

$$\eta = \frac{a_s^2}{S_u^2}\ . \tag{B21}$$

Just ahead of the piston surface,

$$\xi_p = \frac{u_p}{L_p} = 1\ . \tag{B22}$$

From the solution of Eqs. (B17) and (B18), we get z_p and η_p. Using these quantities in the equations given below we calculate u_p and a_p,

$$u_p = \exp(Z_p) \tag{B23}$$

$$a_p^2 = \eta_p u_p^2 \quad . \tag{B24}$$

In addition to u_p (from Eq. (B23)) we also need the pressure at the piston surface which we can get using Eq. (B24) in the following equation,

$$P_p = p_s \left(\frac{a_p}{a_s}\right)^{\frac{2\gamma}{\gamma-1}} \quad . \tag{B25}$$

To complete the solution procedure we still need the fluid velocity, the pressure and the sound speed just behind the shock wave for (Eqs. (B19), (B21) and (B25)). Since we are restricting our attention in this paper to one dimensional flows, we can use normal shock relations to obtain these quantities. The normal shock relations, assuming that γ (the ratio of specific heats) can vary across the shock wave, have been derived in Appendix C.

Appendix C

Flow Conditions across the Shock Wave

Since we are considering only a one-dimensional flow, the flow across the shock wave along any streamline in the three geometries can be obtained from normal shock relations[15]. However, we note that it is important to use the appropriate values for γ, the ratio of specific heats, in the shocked region. Since the normal shock relations are usually obtained assuming γ constant across the shock wave, below we give a brief derivation of the normal shock relations with variable γ.

For an adiabatic, constant area, one-dimensional flow with a normal shock, the equations of continuity, momentum and energy are[15]:

$$\rho_o v_o = \rho_s v_s \tag{C1}$$

$$p_o + \rho_o v_o^2 = p_s + \rho_s v_s^2 \tag{C2}$$

$$h_o + \frac{1}{2} v_o^2 = h_s + \frac{1}{2} v_s^2 , \tag{C4}$$

where the subscript "o" refers to the conditions ahead of the shock wave and the subscript "s" refers to conditions behind the shock wave. We also need an additional constitutive relation to complete the system of equations since there are four unknowns. For a mixture of perfect gases, the caloric equation of state can be written as

$$h = f(p, \rho)$$

$$= \frac{\gamma}{\gamma - 1} \frac{p}{\rho} + h^*_{ref} . \tag{C4}$$

Assuming that the gas mixture is perfect on each side of the shock wave but with different values of γ, we have:

$$h_o = \frac{\gamma_o}{\gamma_o - 1} \frac{p_o}{\rho_o} \tag{C5}$$

and

$$h_s = \frac{\gamma_s}{\gamma_s - 1} \frac{p_s}{\rho_s} . \tag{C6}$$

Eliminating v_s from Eqs. (C1) and (C2), we have:

$$p_s = p_o + \rho_o v_o^2 (1 - R) \tag{C7}$$

where

$$R = \frac{\rho_o}{\rho_s} . \tag{C8}$$

From Eq. (C1) we also have the fluid velocity behind the shock (in the laboratory coordinate system),

$$u_s = v_o - v_s = v_o (1 - R) . \tag{C9}$$

The speed of sound behind the shock is

$$a_s = \left(\frac{\gamma_s p_s}{\rho_s}\right)^{1/2} \quad \text{(C10)}$$

Given the initial conditions (ρ_o, p_o, v_o) ahead of the shock, we can obtain the required parameters p_s, u_s and a_s from Eqs. (C7), (C9) and (C10) if we know the parameter R.

By appropriately combining Eqs. (C1) - (C4) we have obtained the following quadratic equation for R:

$$R^2(1 + \gamma_s) - R(1 + C_1)\, 2\gamma_s + (\gamma_o C_2 + 1)(\gamma_s - 1) = 0 \quad \text{(C11)}$$

where

$$C_1 = \frac{p_o}{\rho_o v_o^2} \quad \text{and} \quad C_2 = \frac{2C_1}{(\gamma_o - 1)} \quad . \quad \text{(C12)}$$

From Eq. (C11), we have

$$R = \frac{\gamma_s(1 + C_1) \pm (\gamma_s^2 (1 + C_1)^2 - (1 + \gamma_s)(\gamma_s - 1)(\gamma_o C_2 + 1))^{1/2}}{(1 + \gamma_s)} \quad \text{(C13)}$$

The importance of using a variable γ for obtaining power-energy relations has been discussed in detail in the main text.

Effect of Temperature on the Ratio of Specific Heats

In order to use the above formulation we need to know the ratio of specific heats both ahead of the shock (γ_o) as well as that behind it (γ_s). In general, these two γ's are different because of differences in the temperature and the mixture composition. For our particular problem the mixture composition may be assumed to be frozen across the shock wave since we are primarily interested in the mixtures up to the time when ignition occurs. In this case the specific heat at constant pressure for the mixture can be written as[16]

$$C_p = \sum_{j=1}^{m} n_j \, (C_p^o)_j \tag{C14}$$

where n_j is in units of the Kg moles of species j per Kg of mixture and $(C_p^o)_j$ is the standard state constant pressure specific heat for species j in J/(Kg mole)(K).

For each species, the specific heat at constant pressure has been given in the form of least square coefficients in Ref. 16 as follows:

$$\frac{(C_p^o)_j}{R} = a_{1_j} + a_{2_j}T + a_{3_j}T^2 + a_{4_j}T^3 + a_{5_j}T^4 \tag{C15}$$

where R is the universal gas constant and is equal to 8314.3 J/(Kg mole)(K). Assuming the mixture behaves like a perfect gas, we can write the ratio of specific heats, γ, as:

$$\gamma = \frac{C_p}{C_p - R} \tag{C16}$$

or to use the data in Ref. 16 more directly,

$$\gamma = \frac{C_p/R}{C_p/R - 1} \quad . \tag{C17}$$

Acknowledgments

The authors greatfully acknowledge suggestions, useful conversations with, and help from Jay P. Boris and T.R. Young. The authors also acknowledge the editorial assistance of Ms. F. Rosenberg. This work has been supported by the Office of Naval Research through the Naval Research Laboratory.

REFERENCES

1. Zeldovich, Y.B., Kogarko, S.M. and Simonov, N.N.: Soviet Phys.-JETP 1, 1689 (1956).
2. Litchfield, E.L., Hay, M.H. and Forshey, D.R.: Ninth Symposium (International) on Combustion, p. 282, Academic Press, 1963.
3. Freiwald, H. and Koch, H.W.: Ninth Symposium (International) on Combustion, p. 275, Academic Press, 1963.
4. Bach, G.G., Knystautas, R. and Lee, J.H.: Thirteenth Symposium (International) on Combustion, p. 1097, The Combustion Institute, 1971.
5. Lee, J.H., Knystautas, R. and Guirao, C.M.: Fifteenth Symposium (International) on Combustion, p. 53, The Combustion Institute, 1975.
6. Knystautas, R. and Lee, J.H.: Combust. Flame 27, 221 (1976).
7. Dabora, E.K.: Effect of Additives on the Lean Detonation Limit of Kerosene Sprays. UCONN0507-129-F, The University of Connecticut, 1980.
8. Dabora, E.K.: The Relation between Energy and Power for Direct Initiation of Hydrogen-Air Detonations. Presented at the Second International Workshop on the Impact of Hydrogen on Water Reactor Safety, Albuquerque, New Mexico, Oct. 1982.

9. Abouseif, G.E. and Toong, T.Y.: Combust. Flame 45, 39 (1982).

10. Taylor, G.I.: Proc. Roy. Soc. A. 186, 273 (1946).

11. Chu, B.-T.: NACA TN 3411, 1955.

12. Urtiew, P.A. and Oppenheim, A.K.: Eleventh Symposium (International) on Combustion, p. 665, The Combustion Institute, 1967.

13. Edwards, D.H., Thomas, G.O. and Williams, T.L.: Combust. Flame 43, 187 (1981).

14. Kailasanath, K. and Oran, E.S.: The Relation Between Power and Energy in the Shock Initiation of Detonations - II. Application to Hydrogen - Air Mixtures. NRL Memorandum Report (in preparation, 1983).

15. Liepmann, and Roshko: Elements of Gasdynamics, John Wiley and Sons, Inc., New York, NY, 1957.

16. Gordon, S. and McBride, B.J.: Computer - Program for Calculation of Complex Chemical Equilibrium Compositions, Rocket Performance, Incident and Reflected Shocks, and Chapmann-Jouguet Detonations. NASA SP-273, 1976. N-78-17724/3.